Supporting information for: Impact of the Organic Cation on the Optoelectronic Properties of Formamidinium Lead Triiodide

Christopher L. Davies,[†] Juliane Borchert,[†] Chelsea Q. Xia,[†] Rebecca L. Milot,[†,‡] Hans Kraus,[¶] Michael B. Johnston,[*,†] and Laura M. Herz[*,†]

[†]*Department of Physics, University of Oxford, Clarendon Laboratory, Parks Road, Oxford OX1 3PU, United Kingdom*

[‡]*Department of Physics, University of Warwick, Gibbet Hill Road, Coventry, CV4 7AL, United Kingdom*

[¶]*Department of Physics, University of Oxford, Denys Wilkinson Building, Keble Road, Oxford OX1 3RH, United Kingdom*

E-mail: michael.johnston@physics.ox.ac.uk; laura.herz@physics.ox.ac.uk

Terahertz Spectroscopy

Supporting Figure S1 shows a schematic of the terahertz spectroscopy setup used to measure the absorption and photoconductivity of $FAPbI_3$. For terahertz time domain spectroscopy (THz-TDS) measurements of phonon modes, the signal from the balanced photodiodes were recorded using a box-car method based on a custom-built analogue to digital converter. For optical pump terahertz probe measurements of photoconductivity, a double lockin technique was used. The optical chopper frequencies were set to 2.5 kHz for the "probe" beam and 125 Hz for the "pump" beam.[S1]

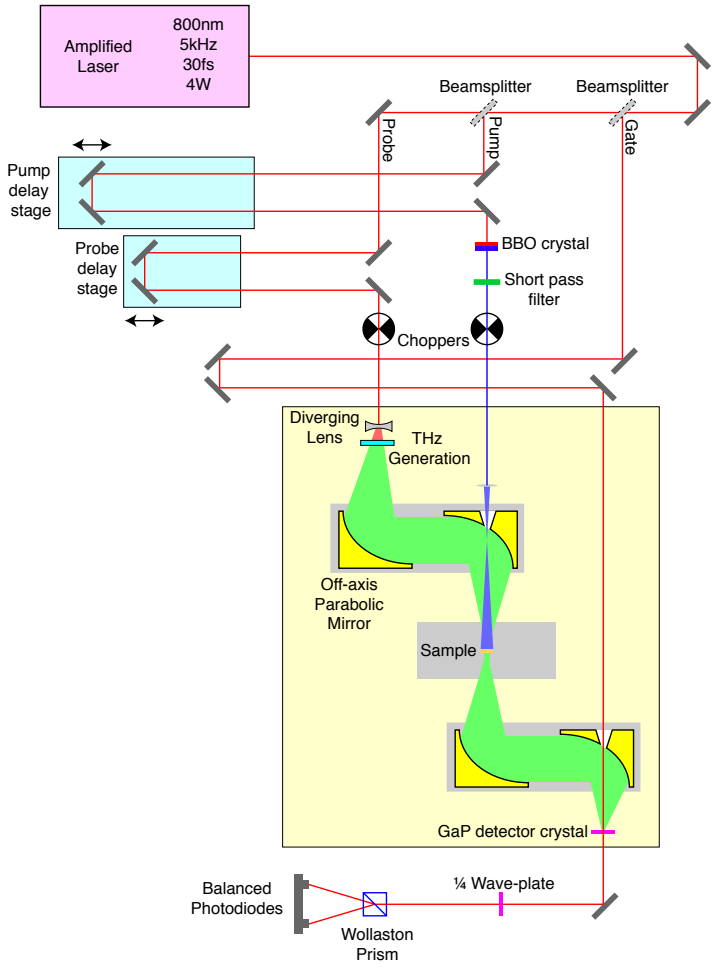

Figure S1: Optical Pump Terahertz Probe Spectroscopy Setup

Photoconductivity of Intra-Excitonic Transitions

Excitonic states in semiconductors consist of discrete bound states and a continuum of unbound states analogous to a Hydrogenic system. The photoconductivity response, $\Delta\sigma$, of transitions from the 1s state to np states and continuum states is described, as a function of angular frequency ω, by the sum of Lorentz oscillators with an oscillator strength given by Fermi's Golden Rule.[S2–S4] The photoconductivity of intra-excitonic transitions is given by:

$$\Delta\sigma(\omega) \propto -i\omega\epsilon_0 \left(\sum_{n=2}^{\infty} \frac{f_{1s\rightarrow np}}{\omega_n^2 - \omega^2 - i\omega\Gamma} + \int_{E_X/\hbar}^{\infty} \frac{f_{1s\rightarrow\infty}(\omega')d\omega'}{\omega'^2 - \omega^2 - i\omega\Gamma} \right) \tag{1}$$

where Γ is a broadening parameter, ϵ_0 is the permittivity of vacuum, ω_n is the transition energy, and $f_{1s\rightarrow np}$ and $f_{1s\rightarrow\infty}$ are the oscillator strengths for the 1s $\rightarrow$ np and 1s $\rightarrow \infty$ transitions, respectively. The transition energy is given by:

$$\omega_n = \frac{E_X}{\hbar}\left(1 - \frac{1}{n^2}\right) \tag{2}$$

where E_X is the exciton binding energy. The oscillator strengths are determined using Fermi's Golden Rule:

$$f_{i\rightarrow f} = \frac{2\pi}{\hbar}(E_f - E_i) \mid \langle\psi_f|\hat{x}|\psi_i\rangle \mid^2 \tag{3}$$

where subscripts i and f denote the initial and final states. The matrix elements for bound and unbound states have been evaluated by Hee-Won Lee[S3] and yield oscillator strengths given by:

$$f_{1s\rightarrow np} = 2\pi\omega_n \left(2^4 n^{7/2} \frac{(n-1)^{n-5/2}}{(n+1)^{n+5/2}} \right)^2 \tag{4}$$

and

$$f_{1s\rightarrow\infty}(\omega) = 2\pi\omega \frac{2^4}{\sqrt{3}(1+x^2)^{5/2}} \frac{e^{-\frac{2}{x}\tan^{-1}(x)}}{(1-e^{-2\pi/x})^{1/2}} \tag{5}$$

where $x = \sqrt{\hbar\omega/E_X - 1}$. The contribution to the photoconductivity for transitions to the continuum states is negligible, and we fit for the contributions from $n = 1$ to $n = 40$ states.

Photoconductivity Measured by Optical Pump Terahertz Probe Spectroscopy (OPTPS)

Here, we provide a derivation for deducing the photoconductivity of a material using OPTPS.[S5] To allow extraction of the photoconductivity, a suitable reference measurement with respect to the sample of interest needs to be considered. As with most nanoscale materials, fabrication of a free standing film is beyond the current methods available and films were therefore grown on a substrate. Figure S2 shows the transmission of a terahertz pulse through (**a**) a reference substrate of thickness L, (**b**) a sample of thickness d on a reference substrate, and (**c**) a photoexcited sample on a substrate.

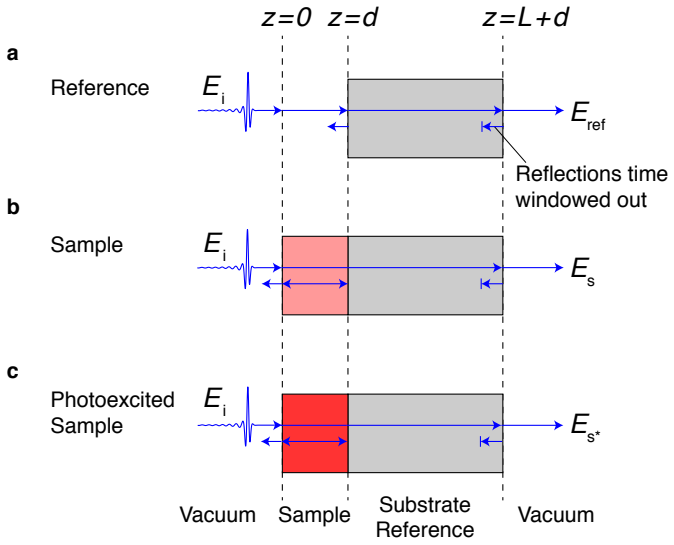

Figure S2: Transmission of a terahertz pulse through: **a** a reference; **b** a sample on a substrate; and **c** a photoexcited sample on a substrate. The reference substrate has thickness L and the sample has thickness d.

Consider an incident propagating monochromatic wave, $E_{\rm i} = E_0 e^{i(kz-\omega t)}$ with a dispersion relation $k = \tilde{n}\omega/c$ where $\tilde{n}$ is the complex refractive index of a material. The transmitted electric fields E for cases **a**, **b** and **c** in the *frequency* domain are given by:

$$E_{\rm ref} = t_{\rm v,r}\, t_{\rm r,v}\, e^{i(\tilde{n}_{\rm v} d + \tilde{n}_{\rm r} L)\omega/c} E_{\rm i} \tag{6}$$

$$E_{\mathrm{s}} = t_{\mathrm{v,s}}\, t_{\mathrm{s,r}}\, t_{\mathrm{r,v}}\, \mathrm{FP}_{\mathrm{vsr}} e^{i(\tilde{n}_{\mathrm{s}} d + \tilde{n}_{\mathrm{r}} L)\omega/c} E_{\mathrm{i}} \tag{7}$$

$$E_{\mathrm{s}^*} = t_{\mathrm{v,s}^*}\, t_{\mathrm{s}^*,\mathrm{r}}\, t_{\mathrm{r,v}}\, \mathrm{FP}_{\mathrm{vs}^*\mathrm{r}} e^{i(\tilde{n}_{\mathrm{s}^*} d + \tilde{n}_{\mathrm{r}} L)\omega/c} E_{\mathrm{i}} \tag{8}$$

where the subscripts v, r and s denote vacuum, reference and sample, $t_{i,j} = 2\tilde{n}_i/(\tilde{n}_i + \tilde{n}_j)$ is the Fresnel transmission at the boundary between materials i and j. FP_{ijk} is the Fabry-Pérot term that is the contribution from multiple internal reflections in material j situated between i and k, and is defined by:

$$\mathrm{FP}_{ijk}(\omega) = \sum_{p=0}^{N} (r_{jk} r_{ji} \exp(2i\tilde{n}\omega d/c))^p \tag{9}$$

where $r_{ij} = (\tilde{n}_i - \tilde{n}_j)/(\tilde{n}_i + \tilde{n}_j)$ are the Fresnel reflection coefficients and N is the number of Fabry-Pérot echos.

The change in transmission of a material upon photoexcitation with respect to the transmission of a sample in the dark, $\Delta T/T$, is defined by:

$$\frac{\Delta T}{T} = \frac{E_{\mathrm{s}^*} - E_{\mathrm{s}}}{E_{\mathrm{s}}} = \frac{E_{\mathrm{s}^*}}{E_{\mathrm{s}}} - 1 \tag{10}$$

For thin film samples ($\omega d/c \ll 1$) the number of Fabry-Pérot echoes can be assumed to tend to infinity ($N \to \infty$) and we can make the approximation $e^{\pm in\omega d/c} = 1 \pm in\omega d/c$. Hence, in the thin-film limit and after some rearrangement the Equation 10 becomes:

$$\frac{\Delta T(\omega)}{T(\omega)} = \frac{i\omega d}{c} \frac{\tilde{n}_{\mathrm{s}^*}^2 - \tilde{n}_{\mathrm{s}}^2}{1 + \tilde{n}_{\mathrm{r}}} \tag{11}$$

The squared complex refractive indices may be written in terms of the dielectric function $\Delta\epsilon = \tilde{n}_{\mathrm{s}^*}^2 - \tilde{n}_{\mathrm{s}}^2$, and hence in terms of photoconductivity $\Delta\sigma = -i\epsilon_0\omega\Delta\epsilon$. Making this substitution and rearranging gives the photoconductivity:

$$\Delta\sigma(\omega) = -\frac{\epsilon_0 c(1 + \tilde{n}_r)}{d} \frac{\Delta T}{T} \tag{12}$$

Extraction of Charge-Carrier Mobility from Optical Pump Terahertz Probe Spectroscopy

The effective mobility of charge carriers $\phi\mu$ is given by:[S6]

$$\phi\mu = \frac{\Delta S}{e n_{\text{eff}}} \tag{13}$$

where ϕ is the excitation-photon-to-generated-free-charge branching ratio, which is, in this case, mostly determined by the ratio of bound (excitonic) to unbound electron and hole pairs generated. $\Delta S = \Delta\sigma d$ is the sheet conductivity, and n_{eff} the effective areal density of charge carriers, which takes into account the Gaussian profiles of the optical pump beam that excites charge carriers and the terahertz probe beam have Gaussian profiles. The effective areal charge carrier density is calculated by:

$$n_{\text{eff}} = \frac{E_{\text{pulse}}}{E_{\text{photon}}} \frac{1}{A_{\text{eff}}} (1 - R)(1 - T) \tag{14}$$

where E_{pulse} and E_{photon} are the energies of the pump pulse and that of the photons (with wavelength of 400 nm). R and T are the reflection and transmission coefficients at the wavelength of 400 nm. The effective area, A_{eff} is given by:

$$A_{\text{eff}} = \int_0^{\infty} \int_0^{2\pi} G(\zeta_{\text{pump}}; r) G(\zeta_{\text{probe}}; r) r dr d\theta \tag{15}$$

where $G(r)$ are gaussian functions with full width half maxima of the pump (ζ_{pump}) and the (ζ_{probe}) beams. Evaluating A_{eff} gives:

$$A_{\text{eff}} = \frac{\pi}{4 \ln 2} \left(\zeta_{\text{pump}}^2 + \zeta_{\text{probe}}^2 \right) \tag{16}$$

Substituting these expressions into Equation 13 gives:

$$\phi\mu = \left(-\epsilon_0 c(1+\tilde{n}_\mathrm{r})\frac{\Delta T}{T}\right)\,\frac{1}{e}\,\frac{E_\mathrm{photon}}{E_\mathrm{pulse}}\frac{\pi}{4\ln 2}\frac{\zeta^2_\mathrm{pump}+\zeta^2_\mathrm{probe}}{(1-R)(1-T)} \tag{17}$$

Modelling Of The Absorption Onset (Elliott Theory)

In this work we have used Elliott's model for the intensity of optical absorption by excitons.[S7] The absorption model is a linear combination of the absorption to bound excitons and electron-hole continuum states. For a direct semiconductor, the absorption coefficient, α, can be written as a function of energy, E, given by:

$$\alpha(E) = b_0 \frac{|\langle \Psi_c | P | \Psi_v \rangle|^2}{E} \left(\sum_{n=1}^{\infty} \frac{4\pi E_{\mathrm{X}}^{3/2}}{n^3} \delta\left(E - \left(E_{\mathrm{G}} - \frac{E_{\mathrm{X}}}{n^2} \right) \right) + \frac{2\pi \sqrt{\frac{E_{\mathrm{X}}}{E - E_{\mathrm{G}}}}}{1 - \exp\left(-2\pi \sqrt{\frac{E_{\mathrm{X}}}{E - E_{\mathrm{G}}}} \right)} c_0^{-1} \mathrm{JDoS}(E) \right) \tag{18}$$

where E_{G} is the band gap energy, E_{X} is the exciton binding energy, b_0 is a proportionality constant, $\delta(E)$ is the Dirac delta function, and c_0 is a joint density of states constant given below by Equation 20. The joint density of states (JDoS) is given by,

$$\mathrm{JDoS}(E) = \begin{cases} c_0 \sqrt{E - E_{\mathrm{G}}}, & \text{for } E > E_{\mathrm{G}} \\ 0, & \text{otherwise} \end{cases} \tag{19}$$

where,

$$c_0 = \frac{1}{(2\pi)^2} \left(\frac{2\mu}{\hbar^2} \right)^{3/2} \times 2 \ . \tag{20}$$

where μ is the reduced effective mass of electron-hole system.

Electron-phonon interactions broaden the absorption, with larger effects at higher temperatures.[S8] An additional energetic disorder may lead to some element of inhomogeneous broadening. We found that a log-normal distribution was useful to parameterise this additional disorder brought into the system. Previous studies have found a distribution of band gap positions varying with crystallite size and even within a single crystal.[S9,S10] Our model can be described as the sum of the contributions of excitonic and continuum states convolved

with a broadening function. The broadening function is a normalised function centred at the maximum and is the convolution of a normal distribution, caused by electron-phonon coupling, and a log-normal distribution, caused by disorder and local fluctuations of the stoichiometry of the material. In mathematical notation,

$$g(E) = \mathcal{N}(0,\, \sigma_T^2) \otimes \ln\big(\mathcal{N}(u_\mathrm{s},\, \sigma_\mathrm{s}^2)\big)\ , \tag{21}$$

where $\otimes$ represents a convolution, the subscript T denotes temperature dependent variables, $\mathcal{N}(u_N,\, \sigma_N^2)$ is a Normal distribution with mean u_N and variance σ_N^2, and $\ln(\mathcal{N}(u, \sigma^2))$ is a Log-normal distribution. u_s and σ_s are fitted globally and σ_T are temperature dependent parameters fitted for each temperature representing the electron-phonon coupling.

Absorption Coefficient Comparison of $FAPbI_3$ and $MAPbI_3$

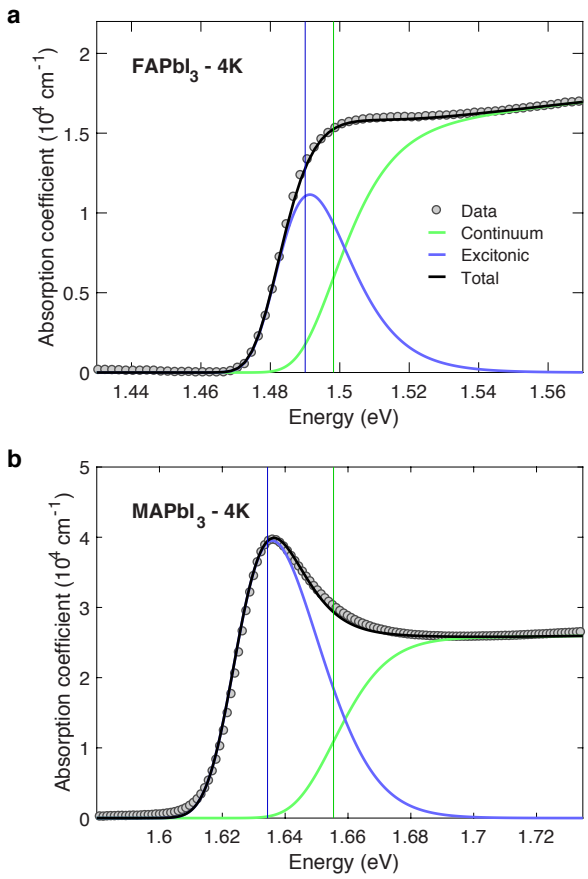

Figure S3: Absorption coefficient of (**a**) $FAPbI_3$ and (**b**) $MAPbI_3$ at 4 K. Absorption coefficient of $MAPbI_3$ taken from Ref. S11. Absorption spectra at 4 K, measured by Fourier transform infrared (FTIR) spectroscopy. Experimental data are shown as grey circles and a fit based on Elliott's theory is shown as a solid black line. Contributions to the absorption coefficient from bound excitonic and continuum states are displayed by blue and green lines, respectively. The vertical green lines show the band gap energy, E_G and the difference between blue and green vertical lines are the exciton binding energies, E_X. Note that the displayed ranges of x-axes have been chosen such that the band-gaps of the materials are aligned, for ease of comparison. Fits to these data based on Elliott Theory, as described in the section above, yield values of $E_G = 1.50\,\text{eV}$ and $E_X = 8.1\,\text{meV}$ for $FAPbI_3$ and $E_G = 1.66\,\text{eV}$ and $E_X = 21\,\text{meV}$ for $MAPbI_3$.

Exciton Binding Energy from Absorption fitting

Here we address the disparity between the exciton binding energy measured from OPTPS (5.3 meV at 10 K) and the exciton binding energy extracted from absorption spectra modelling ($\sim$ 8 meV at 10 K). Supporting Figure S4 shows the absorption data and absorption model using the fitted exciton binding energy, E_X, and also $E_X \pm 3$ meV. The band gap was shifted by the same energy as the exciton binding energy, such that the energy of the 1s state was unchanged, and hence all models had the same absorption onset energy. The model was normalised to the data at an energy above the band gap shown by the intersection of the three lines in each plot. Larger exciton binding energies give a more pronounced exciton peak and a flatter absorption spectrum above the band gap. We see that the model assumes a negative curvature above the band gap for all values of exciton binding energies, mostly as a result of the dependence of the density of states on the square root of the above-gap energy, for a direct semiconductor. However, the opposite is true for the measured absorption spectra, which produces a positive curvature above the band gap. The contrasting curvature of Elliott theory and absorption spectra at energies greater than 100 meV above the band gap for $FAPbI_3$ could be the cause of the difference in measurement of the exciton binding energy between OPTPS and absorption spectra. As we have argued recently, such divergences may arise because Elliott's theory does not account for the possible presence of multiple electronic transitions, non-parabolic bands and an energy dependence of the associated matrix elements.[S11] As a result, the shape of the free (uncorrelated) continuum-state absorption may deviate from the square-root dependence on energy above the gap.

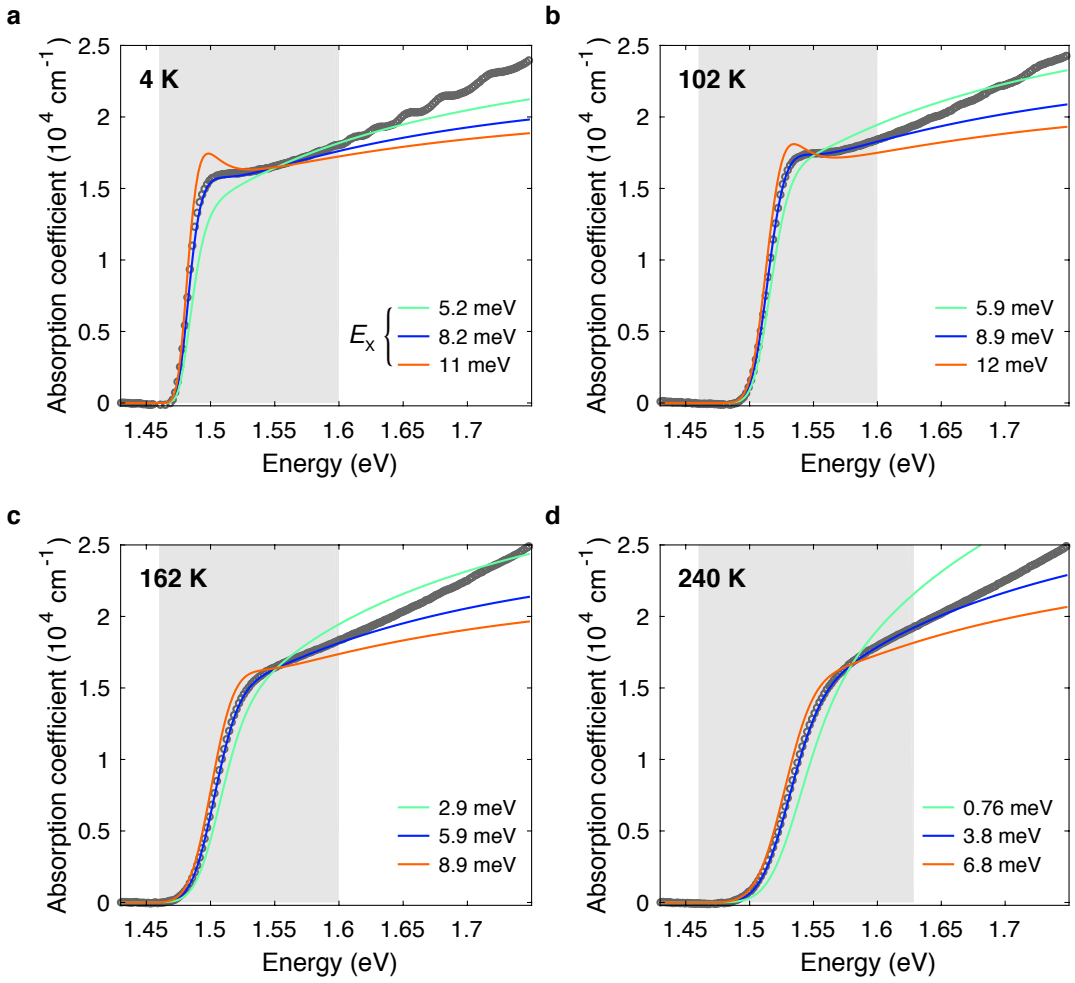

Figure S4: Absorption onset modelling for a thin film of $FAPbI_3$. **a-d** Absorption coefficient at 4 K, 102 K, 162 K and 240 K. The grey area shows the data used to model the absorption. The blue line shows the fit to the data. The green and orange lines show fits with the exciton binding energy adjusted by ±3 meV. The band gap was adjusted by the same amount such that the 1s state of the exciton is at the same energy for all three fits (blue, green orange).

Fluence-dependent Photoconductivity of $FAPbI_3$ at 1.7 K

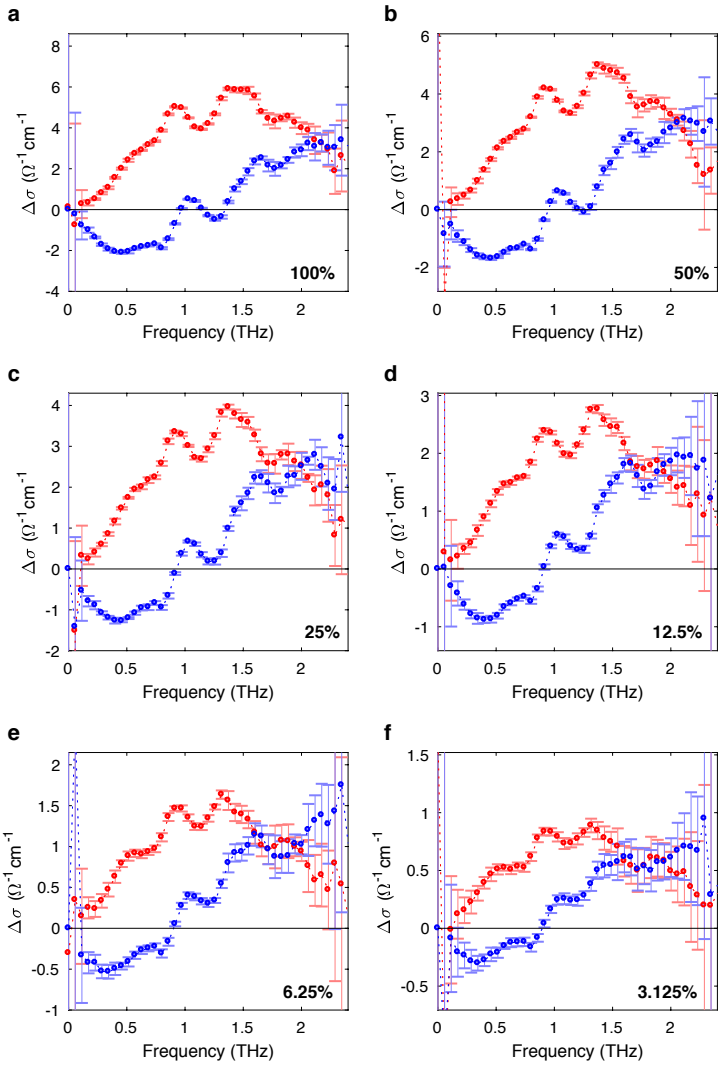

Figure S5: Fluence-dependent photoconductivity of a thin film of $FAPbI_3$ at 1.7 K. **a-f** Photoconductivity of $FAPbI_3$ measured at a pump power corresponding to 100, 50, 25, 12.5, 6.25, 3.125 percent of the maximum pump power (3 mW), respectively. The photoconductivity was measured using the magneto-OPTPS system as described in the main text, with zero magnetic field.

References

(S1) Milot, R. L.; Eperon, G. E.; Snaith, H. J.; Johnston, M. B.; Herz, L. M. *Adv. Funct. Mater.* **2015**, *25*, 6218–6227.

(S2) Kaindl, R. A.; Hägele, D.; Carnahan, M. A.; Chemla, D. S. *Phys. Rev. B* **2009**, *79*, 45320.

(S3) Lee, H.-W. *Publications of The Korean Astronomical Society* **2007**, *22*, 21–33.

(S4) Luo, L.; Men, L.; Liu, Z.; Mudryk, Y.; Zhao, X.; Yao, Y.; Park, J. M.; Shinar, R.; Shinar, J.; Ho, K.-M.; Perakis, I. E.; Vela, J.; Wang, J. *Nat. Commun.* **2017**, *8*, 15565.

(S5) Joyce, H. J.; Boland, J. L.; Davies, C. L.; Baig, S. A.; Johnston, M. B. *Semicond. Sci. Technol.* **2016**, *31*, 103003.

(S6) Wehrenfennig, C.; Eperon, G. E.; Johnston, M. B.; Snaith, H. J.; Herz, L. M. *Adv. Mater.* **2014**, *26*, 1584–1589.

(S7) Elliott, R. J. *Phys. Rev.* **1957**, *108*, 1384.

(S8) Wright, A. D.; Verdi, C.; Milot, R. L.; Eperon, G. E.; Pérez-Osorio, M. A.; Snaith, H. J.; Giustino, F.; Johnston, M. B.; Herz, L. M. *Nat. Commun.* **2016**, *7*, 11755.

(S9) Draguta, S.; Thakur, S.; Morozov, Y. V.; Wang, Y.; Manser, J. S.; Kamat, P. V.; Kuno, M. *J. Phys. Chem. Lett.* **2016**, *7*, 715–721.

(S10) Grancini, G.; Srimath Kandada, A. R.; Frost, J. M.; Barker, A. J.; De Bastiani, M.; Gandini, M.; Marras, S.; Lanzani, G.; Walsh, A.; Petrozza, A. *Nat. Photon.* **2015**, *9*, 695–701.

(S11) Davies, C. L.; Filip, M. R.; Patel, J. B.; Crothers, T. W.; Verdi, C.; Wright, A. D.; Milot, R. L.; Giustino, F.; Johnston, M. B.; Herz, L. M. *Nat. Commun.* **2018**, *9*, 293.